INTERNATIONAL JOURNAL FOR NUMERICAL METHODS IN FLUIDS, VOL. 20, 1047–1059 (1995)

INVESTIGATION OF GENERALIZED FLUX VECTOR SPLITTING FOR COMPRESSIBLE FLOWS ON TRIANGULAR MESHES

BRUNO STOUFFLET

Dassault Aviation, 78 Quai Marcel Dassault, F-92214 Saint-Cloud, France

SUMMARY

The paper presents some investigations in developing schemes based on a splitting of the Euler equations into a pure convective part and an acoustic part (pressure term) combined with a multidimensional treatment on unstructured triangular meshes. Two decompositions are considered and are compared with classical approaches on two-dimensional inviscid flow simulations.

KEY WORDS generalized flux vector; triangular meshes; inviscid flow

1. INTRODUCTION

In the past years intensive research on computational fluid dynamics has been devoted to the development and use of numerical discretizations of systems of conservation laws using upwind formulations. Current methods are based on one-dimensional arguments as approximate Riemann solvers and thus suffer from excessive dissipation (see e.g. References 1–3). On unstructured meshes made of triangles or tetrahedra one can benefit from specific properties even though higher-order approximations based on one-dimensional first-order concepts can have desired properties (preserving linearity). Attempts at multidimensional formulations have become truly successful these last two years (see Reference 4 for an enlightening review and Reference 5 and 6 for some achieved formulations). The extension to systems still requires some improvements and remains somewhat unnatural (simple wave decomposition). An intensive activity has arisen on that research topic.

Meanwhile, approximation schemes based on a splitting of the Euler equations into a pure convective part and an acoustic part (pressure term) have been proposed and have proved to be very promising for compressible flow computations. The main contributions in this direction are the upwind flux-splitting scheme AUSM developed by Liou[7] and the related CUSP formulation proposed recently by Jameson,[8] as well as an earlier formulation[9] combining some SUPG approximation for the convective terms with a centred approximation of the pressure term. This paper deals with the investigation of combining some AUSM-type formulation with a multidimensional treatment on unstructured triangular meshes. The idea is to treat the pure convective term of the AUSM approach as a set of *scalar* convection equations where the velocity acts as the convective vector. One can then apply some of the accurate scalar advective schemes. Distributive schemes proposed in Reference 5 which are second-order-accurate, non-oscillatory and have compact stencils can be chosen. The pressure term is treated independently.

Two decompositions will be considered giving two flux vector splittings. Results of subsonic bidimensional flows around aerofoil profiles computed with this new approach will be compared with those obtained with classical approaches. Particular attention will be devoted to entropy deviation to identify the accuracy of this method.

CCC 0271–2091/95/091047–13

2. LAGRANGE–GALERKIN FORMULATION

For the sake of simplicity we shall consider bidimensional spatial discretizations, but most of the ideas presented here can be extended to 3D. The following models will be under consideration:

$$\textit{conservation law} \quad w_t + \vec{\nabla}(\vec{f}(w)) = 0, \quad w \in \mathbb{R}, \tag{1}$$

$$\textit{hyperbolic system} \quad W_t + \vec{\nabla} \cdot \vec{F}(W)) = 0, \quad W \in \mathbb{R}^d, \quad d \geq 1. \tag{2}$$

Let $\mathcal{T}$ be a triangulation of the computational domain $\Omega \subset \mathbb{R}^2$ with boundary Γ of unit normal $\vec{v}_\Gamma$. We denote by T a current element, in the case of a triangle by $\vec{n}_i^T$ the inward integrated normal opposite to node N_i, by $K(i)$ the set of neighbouring nodes of node N_i and by supp(i) the support of the basis function ϕ_i associated with node N_i. Let V_h^d be a set of piecewise polynomial functions from $\mathbb{R}^2$ with values in $\mathbb{R}^d$ that are continuous. Further, the basis of V_h^d is the set of functions ϕ_j satisfying the Lagrange interpolation conditions. Let us consider the following abstract family of schemes for the spatial approximation of the hyperbolic system (2):

$$\int_\Omega W_t \phi \mathrm{d}v + \int_\Omega \phi \nabla \cdot \vec{F}(W) \mathrm{d}v = 0, \tag{3}$$

where $\vec{F}(W)$ is considered as an element of V_h^d (group representation) and ϕ is a test function. The spatial scheme is then described as

$$\int_\Omega \frac{W^{n+1} - W^n}{\Delta t} \phi \mathrm{d}v + \int_\Omega \phi \nabla \cdot \vec{F}(W^n) \mathrm{d}v = 0. \tag{4}$$

This scheme reduces to the Euler forward time integration, but it is not explicit when the Lagrange–Galerkin mass matrix is not diagonal. However, a mass-lumped variant can prove to be interesting, which is written at each node N_i as

$$\left(\sum_j \int_\Omega \phi_i \phi_j \mathrm{d}v \right) \frac{W_i^{n+1} - W_i^n}{\Delta t} + \int_\Omega \phi \nabla \cdot \vec{F}(W^n) \mathrm{d}v = 0. \tag{5}$$

As far as structured meshes are concerned, a stability result (CFL condition) can easily be found by Fourier analysis. Schemes (4) and (5) have been tried by many authors for P_1 or Q_1 elements. A very short P_2 experiment is also presented in Reference 10.

3. FINITE VOLUME GALERKIN

We first notice that Lagrange–Galerkin methods may be interpreted as finite volume schemes in some extended sense; indeed, the divergence operator can be written as (boundary terms excluded)

$$(\vec{\mathcal{M}}\vec{\mathcal{F}})_i = \sum_j \frac{1}{2} \int (\phi_i \vec{\nabla} \phi_j - \phi_j \vec{\nabla} \phi_i) \vec{\mathcal{F}}_j \mathrm{d}v = \sum_j \vec{\mathcal{M}}_{ij} \vec{\mathcal{F}}_j. \tag{6}$$

It is easy to check that $\{\vec{\mathcal{M}}\}$ is a skew matrix; note that all the diagonal elements of such a matrix are necessarily equal to zero ($\vec{\mathcal{M}}_{ii} = 0, \forall i$). Furthermore, since constant vectors belong to the kernel of $\{\vec{\mathcal{M}}\}$, we have

$$\sum_j \vec{\mathcal{M}}_{ij} = 0, \quad \forall i; \quad \text{thus} \sum_j \vec{\mathcal{M}}_{ij} \vec{\mathcal{F}}_j = \sum_j 2 \vec{\mathcal{M}}_{ij} \frac{\vec{\mathcal{F}}_i + \vec{\mathcal{F}}_j}{2}.$$

The right-hand side is a finite volume flux integration between node N_i and node N_j with the following *mean normal vector* (elementary flux):

$$(\eta_{ij}^x = \int \left(\phi_i \frac{\partial \phi_j}{\partial x} - \phi_j \frac{\partial \phi_i}{\partial x} \right) \mathrm{d}v \qquad \eta_{ij}^y = \int \left(\phi_i \frac{\partial \phi_j}{\partial y} - \phi_j \frac{\partial \phi_i}{\partial y} \right) \mathrm{d}v. \tag{7}$$

Further, we recognize a centred difference integration, since a pure arithmetic mean is taken between $\{\mathscr{F}\}_i$ and $\{\mathscr{F}\}_j$. Let us write the above scheme (5) with H_i denoting the flux term

$$H_i = \sum_{j \neq i} \Phi^{\text{centred}}(W_i, W_j, \vec{\eta}_{ij}) + \int_\Gamma \vec{F}(W) \cdot \vec{v}_\Gamma^0 \phi_i \mathrm{d}\sigma. \tag{8}$$

Lemma 1

For any Galerkin approximation with Lagrange continuous interpolation on the divergence operator, an equivalent finite volume formulation can be expressed as a relation on fluxes between a given degree of freedom and its neighbours:

$$\int \phi_i \nabla \cdot \vec{F} \approx \sum_{j \neq i} \frac{\vec{F}_i + \vec{F}_j}{2} \cdot \vec{\eta}_{ij}.$$

Instead of applying a centred difference scheme to evaluate the fluxes, one may consider a Riemann problem with w_i and w_j as left and right states and $\vec{\eta}_{ij}$ for defining the interface (normal to $\vec{\eta}_{ij}$). Let us notice that the projection of fluxes on the $\vec{\eta}_{ij}$-direction reduces the problem to the one-dimensional case. Then a Godunov extension of the Lagrange–Galerkin scheme can be defined as

$$(\vec{\mathscr{M}}\vec{\mathscr{F}})_i = \sum_{j \neq i} \Phi^{\text{Riemann}}(W_i, W_j, \vec{\eta}_{ij}). \tag{9}$$

Lemma 2

In the case of an advection equation (1) with $\vec{f}(w) = \vec{V} \cdot \Lambda w$, the whole family of upwind Lagrange–Galerkin schemes satisfies the positivity preservation when advanced with the mass-lumped RK1 scheme under the following CFL condition:

$$d_i - \Delta t \sum_{j \neq i} \vec{V}_{ij} \cdot \vec{\eta}_{ij} \geq 0. \tag{10}$$

Remark 1

In the particular case of linear triangular elements (P_1 approximations) a geometrical interpretation can be given. It has been shown[11,12] that $\vec{\eta}_{ij}$ is the integration of the normal vector between two adjacent cells C_i and C_j if these cells are delimited by the medians of the neighbouring triangles:

$$\vec{\eta}_{ij} = \int_{\partial C_i \cap \partial C_j} \vec{\eta} \mathrm{d}\sigma = \int_{\text{supp}(i) \cap \text{supp}(j)} (\phi_i \vec{\nabla} \phi_j - \phi_j \vec{\nabla} \phi_i) \mathrm{d}v. \tag{11}$$

The resulting scheme can be rewritten as

find $W \in V_h^d$ such that

$$\int_{C_i} \frac{\partial W}{\partial t} \mathrm{d}v + \sum_{j \in K(i)} H_{ij}^{(1)} + \int_{\partial C_i \cap \Gamma} \vec{F}(W) \cdot \vec{v}_\Gamma \mathrm{d}\sigma = 0,$$

where $H_{ij}^{(1)} = \Phi_F(W_i, W_j, \vec{\eta}_{ij})$. The formulation takes the form of looping over each side in the mesh and sending contributions to the appropriate nodes. This gives an *edge-based data structure* which is the most compact that can be used for unstructured meshes. In the following section this formulation will be derived from a finite element Galerkin approximation in the case of *triangular or tetrahedral* elements. In the case of stretched triangles or tetrahedra the angle between the integrated normal vector and the corresponding edge can become very large, which can create excessive numerical diffusion. Studies to investigate new definitions of modified, better-suited cells have given significantly improved results in some test cases.[13] One possible method is to define an 'optimized' dual mesh by a cell construction minimizing the angle between directions of upwinding and edge directions for each element (as sketched in Figure 1(b)). We can notice that both constructions are identical for equilateral triangles, whereas the second one tends towards quadrangular cell type in the case of right-angled triangles (as shown in Figure 1(b)). It can also be observed that the centred part and the dissipative part of the approximate Riemann solver flux can be independently computed using either the Galerkin or the optimized dual mesh, giving a large family of schemes.

Remark 2

Q_1–Lagrange approximations are richer in interpolation and can degenerate easily from 3D to 2D and from 2D to 1D (solutions are identical). For this case we note that $\vec{\eta}_{ij}$ does not rely any more on a tessellation. In particular, beside edges, diagonals of quadrilaterals also support flux integration.

Remark 3

In all the above approaches, boundary integrals over Γ are computed in order to take into account the physical boundary conditions.

4. MUSCL EXTENSIONS

We describe now extensions of previous schemes to second-order accuracy. They can be viewed as perturbation of the finite element scheme by (essentially) a numerical viscosity in terms of fourth-order derivatives. Indeed, following van Leer,[14] we can replace in the approximate Riemann solver the nodal values W_i and W_j by higher-order interpolations:

$$H_{ij}^{(2)} = \Phi_F{}^{\text{first,upwind}}(W_{ij}, W_{ji}, \vec{\eta}_{ij}), \quad \text{with } W_{ij} = W_i + \nabla W_{ij} \cdot \frac{\overrightarrow{N_i N_j}}{2},$$

where ΔW_{ij} is an approximation of ΔW at node N_i. Several choices are possible (see Reference 15 for the P_1 case). In order to possibly obtain a fully upwind scheme, we suggest the 'upwind element construction',[16] where W_{ij} and W_{ji} are values at the interface ∂C_{ij} which have been interpolated by using upwind gradients as described below.

We define the downstream and upstream triangles T_{ij} and T_{ji} for each segment $[N_i, N_j]$ as shown in Figure 2. Let the centred gradient be $\Delta W_{ij} = \Delta W|_{T_{ij}^{\beta}}$, where T_{ij}^{β} is one of the triangles having N_i and N_j as vertices.

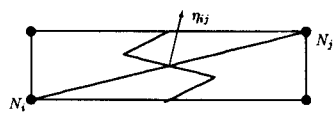

Figure 1(a). Classical Galerkin cell

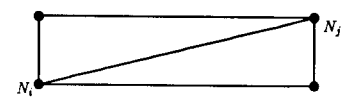

Figure 1(b). Modified cell definition

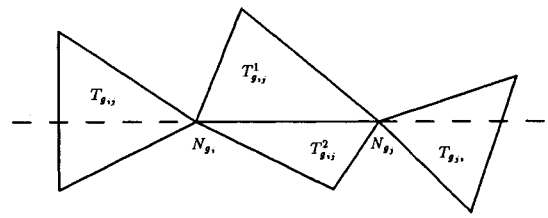

Figure 2. Downstream and upstream triangles for the segment $[N_i, N_j]$

A good procedure in terms of accuracy is to use limiters on characteristic variables. We compute these variables by the transformation taken at the segment's midpoint. If we denote by Π_{ij} the eigenvector matrix corresponding to the flux, then the values at the interface needed to compute the flux $H_{ij}^{(2)}$ are given by

$$W_{ij} = W_i + \Pi_{ij} Lc_{ij} \Pi_{ij}^{-1} \left(\frac{1-\kappa}{4} \nabla W|_{Tij} + \frac{1+\kappa}{4} \nabla W_{ij} \right) \cdot \overrightarrow{N_i N_j},$$

where Lc_{ij} and Lc_{ji} are the diagonal limiting matrices introduced to reduce numerical oscillations of the solution and to provide some kind of monotonicity property. We rely on the Van Albada limiter[14] associated with the Fromm scheme corresponding to $\kappa = 0$, combining monotonocity and second-order accuracy.

However, this construction is still rather heuristic in this 2D context and rigorously non-oscillating schemes are hardly derived. We refer to Reference 17 for an attempt at a multidimensional extension of Harten's incremental condition.

5. DISTRIBUTIVE FORMULATIONS

In this section we restrict our analysis to linear finite elements on triangles (P_1). Distributive compact schemes introduced by Struijs *et al.*[5] have proved to give an appropriate frame to derive accurate monotone schemes. Consider a scalar conservation equation. If we come back to the Galerkin formulation given in equation (5) and formally apply the group representation

$$\int_\Omega \phi_i \nabla \cdot \vec{f}(w) \mathrm{d}v = \int_\Omega \phi_i \sum_j \nabla \phi_j \vec{f}_j(w) \mathrm{d}v = \frac{\mathrm{area}(T)}{3} \int_\Omega \nabla \cdot \vec{f}(w) \mathrm{d}v, \tag{13}$$

the mass-lumped variant can then be rewritten in the compact residual distributive formulation

$$V_i \frac{w_i^{n+1} - w_i^n}{\Delta t} - \sum_T \tfrac{1}{3} \Re(\mathrm{T}) = 0, \tag{14}$$

where the residual $\Re(T)$ is given by

$$\Re(\mathrm{T}) = -\int_{\partial \mathrm{T}} \vec{\mathrm{f}} \cdot \vec{\mathrm{n}} = \int_{\mathrm{T}} \vec{\nabla} \cdot \vec{\mathrm{f}}(\mathrm{w}) \mathrm{dv}. \tag{15}$$

Assuming now a continuous piecewise linear approximation of w (P_1 elements), the above formulation suggests defining a general class of distributive scheme of the form

$$V_i \frac{w_i^{n+1} - w_i^n}{\Delta t} - \sum_T \beta_{T,i} R(\vec{\lambda}, T, w) = 0, \quad \text{with} \sum_{i=1}^{3} \beta_{T,i} = 1, \tag{16}$$

where the residual is integrated using the linear representation of w:

$$R(\vec{\lambda}, T, w) = \text{area}(T)\vec{\lambda} \cdot \vec{\nabla} w = \sum_{i=1}^{3} k_i w_i, \tag{17}$$

with

$$\vec{\lambda} = \frac{1}{\text{area}(T)} \int_T \frac{\mathrm{D}\vec{f}}{\mathrm{D}w} \mathrm{d}v, \qquad k_i = \tfrac{1}{2}\vec{\lambda} \cdot \vec{n}_i^T.$$

This formulation has been advocated in References 5 and 18 in order to derive upwind schemes based on advection speed $\vec{\lambda}$ where only downwind nodes receive a contribution. To have simultaneously positive and linearity-preserving approximations, the schemes have to be non-linear. Two particular schemes (the so-called N-scheme which is linear and first-order-accurate and PSI which is non-linear and close to second-order accuracy) constructed in Reference 18 have been selected

$$\beta_{T,i}^{(N)} R(\vec{\lambda}, T, w) = -k_i^+ (w_i - w_{in}^T), \quad \text{with } w_{in}^T = -k_i^+ \left(w_i - \frac{\sum_{j=1}^3 w_j k_j^-}{\sum_{j=1}^3 k_j^-} \right),$$

$$\beta_{T,i}^{(PSI)} R(\vec{\lambda}, T, w) = \frac{k_i^+ ((w_i - w_{in}^T) R(\vec{\lambda}, T, w))^-}{\sum_{j=1}^3 k_j^+ ((w_j - w_{in}^T) R(\vec{\lambda}, T, w))^-} R(\vec{\lambda}, T, w).$$

Remark 4

Whereas boundary conditions are assumed in a weak form through boundary integrals in the previous formulations, no such contribution appears any more in the present approximations (in fact, boundary integrals are part of the boundary elementary flux evaluation). Boundary conditions will then be imposed strongly.

6. GENERALIZED FLUX VECTOR SPLITTING

We have shown that a Lagrange–Galerkin approximation of a general hyperbolic system can be interpreted in other formulations which lead to different integration schemes. In this section we combine the above formulations applied to an adequate splitting of the Euler equations of gas dynamics. Consider the two-dimensional equations of gas dynamics where the state vector and the fluxes are given by

$$W = \begin{pmatrix} \rho \\ \rho u_x \\ \rho u_y \\ \rho E \end{pmatrix} = (W^{(l)}), \qquad F_x = \begin{pmatrix} \rho u_x \\ \rho u_x^2 + p \\ \rho u_y u_x \\ \rho H u_x \end{pmatrix}, \qquad F_y = \begin{pmatrix} \rho u_y \\ \rho u_x u_y \\ \rho u_y^2 + p \\ \rho H u_y \end{pmatrix}.$$

where ρ is the density, $\vec{u} = (u_x, u_y)$ is the velocity, E is the total energy per unit mass, p is the pressure and H is the stagnation enthalpy. If γ is the ratio of specific heats, then

$$\rho = (\gamma - 1)\left(\rho E - \frac{\rho \vec{u}^2}{2} \right), \qquad H = E + \frac{p}{\rho}, \qquad \text{speed of sound } c = \sqrt{\left(\frac{\gamma p}{\rho} \right)}.$$

In a steady flow the stagnation enthalpy H is constant, equal to H_t.

We want to investigate schemes based on a separation of convective and pressure fluxes as

$$\vec{F} = \vec{F}_u + \vec{F}_p,$$

where F_p contains the pressure term only, which have been proposed by Liou[7] and Jameson[8] to derive new upwind concepts. Two decompositions can be considered:

$$\vec{F}_u = \begin{pmatrix} \rho \\ \rho u_x \\ \rho u_y \\ \rho H \end{pmatrix} \vec{u} = G_u \vec{u} \quad \text{or} \quad \vec{F}_u = \begin{pmatrix} 1 \\ u_x \\ u_y \\ E \end{pmatrix} \vec{u} = G_{\rho u} \rho \vec{u}.$$

Firstly we consider the first decomposition with convective speed $\vec{u}$. Since this field is not divergence-free, the derivation rule gives

$$\int_T \vec{\nabla} \cdot \vec{F}_u^{(l)} \mathrm{d}v = \int_T \vec{u} \cdot \nabla G_u^{(l)} \mathrm{d}v + \int_T \nabla \cdot \vec{u} G_u^{(l)} \mathrm{d}v. \tag{19}$$

Applying to the first three scalar equations a distributive scheme as proposed in the previous section, since the variables $G_u^{(l)}$ are assumed to be linear on T, a possible approximation (FVS1) could be

$$\frac{W_i^{(l)^{n+1}} - W_i^{(l)^n}}{\Delta t} + \sum_T \beta_{T,i} R(\vec{\lambda}_u, T, G_u^{(l)}) + \sum_{j \in K(i)} \Phi_{F_p}^{\text{upwind}}(W_{ij}, W_{ji}, \vec{\eta}_{ij}) + \int_T (\nabla \cdot u) G_u^{(l)} \phi_i \mathrm{d}v = 0$$

$$\text{for } l = 1, 3, \tag{20}$$

with

$$\vec{\lambda}_u = \frac{1}{\text{area } (T)} \int_T \vec{u} \mathrm{d}v.$$

Then we use the stagnation enthalpy to update the energy.

In order to work with a divergence-free convection speed, it seems attractive to work with the second decomposition based on ρu. Firstly we replace the energy equation by a pseudo-unsteady equation given by

$$\frac{\partial(\rho H)}{\partial t} = \frac{\partial(\rho H u_x)}{\partial x} + \frac{\partial(\rho H u_y)}{\partial y}.$$

We can now derive a scheme (FVS2) based on convective speed $\rho \vec{u}$ with the state vector $\tilde{W} = (\rho, \rho u_x, \rho u_y, \rho H)^{\mathrm{T}}$ and

$$\vec{\lambda}_{\rho u} = \frac{1}{\text{area } (T)} \int_T \rho \vec{u} \mathrm{d}v :$$

$$\frac{W_i^{(l)^{n+1}} - \tilde{W}_i^{(l)^n}}{\Delta t} + \sum_T \beta_{T,i} R(\vec{\lambda}_{\rho u}, T, G_{\rho u}^{(l)}) + \sum_{j \in K(i)} \Phi_{F_p}^{\text{upwind}}(\tilde{W}_i, \tilde{W}_j, \vec{\eta}_{ij}) = 0 \quad \text{for } l = 2, 4. \tag{21}$$

In this case the update in density is computed via the equation

$$\rho^{n+1} = \frac{(\rho H)^{n+1}}{H_t}.$$

Remark 5

To complete the description of both formulations, one needs to define the approximate flux function $\Phi_{F_p}^{\text{upwind}}$. Following the pressure fluxes proposed by Liou and Jameson, assuming a proper zone of dependence, we chose

$$\Phi_{F_p}^{\text{upwind}}(W_L, W_R, \vec{n}) = p_L^+ + p_R^-, \quad \text{with } p^+ = \frac{p}{2}\left(1 + \frac{\vec{u}\cdot\vec{n}}{c}\right) \text{ in the subsonic region.}$$

7. NUMERICAL RESULTS

As a first investigation we have focused on subsonic test cases to evaluate the behaviour of the above schemes. In all test cases new schemes are compared with a classical upwind scheme (FVG + MUSCL) based on an Osher approximate Riemann solver (called the reference scheme). Firstly, simulations of flow around an NACA 0012 aerofoil are presented. A regular mesh (Figure 3) has been used (3200 nodes). Entropy distributions at the wall are presented in Figure 4(a) for the reference scheme and in Figure 4(b) for the FVS1 + PSI scheme. The overall level of entropy is quite similar. The spurious entropy generation is more confined in the leading edge region for the reference solution than for the second one.

Then a subsonic flow around an RAE 2822 aerofoil is simulated at $M_\infty = 0{\cdot}30$ and $\alpha = 2°$. A rather coarse mesh (1200 nodes with an aspect ratio of 200 near the body) is first considered. A solution obtained with FVS1 + N (Figure 5(b)) is compared with the reference one (Figure 4(a)). In both solutions spurious entropy is generated in the leading edge region, whereas the splitting scheme gives a better level at the windward side. A similar entropy level is present in the strong expansion of the leeward side.

The same test case is then performed using a fine mesh aimed at computing viscous flows (Figure 6). The mesh aspect ratio is more than 1000 in the first layer of boundary elements. Four solutions are presented, obtained respectively with the reference scheme (Figures 7(a) and 8(a)), FVS1 + N (Figures 7(b) and 8(b)), FVS1 + PSI (Figures 7(c) and 8(c)) and FVS2 + PSI (Figures 7(d) and 8(d)). Globally

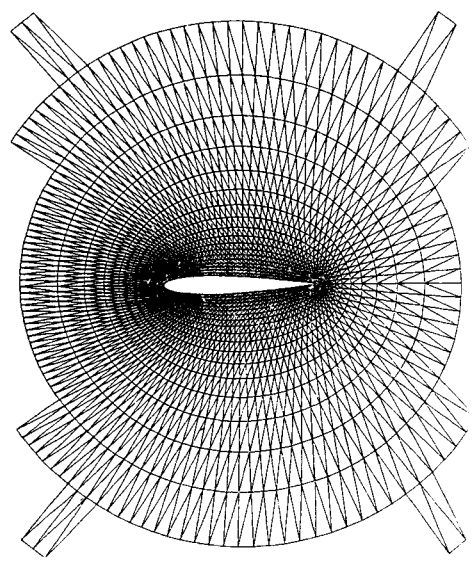

Figure 3. NACA 0012 aerofoil grid

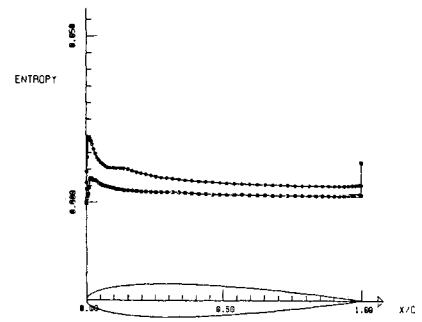

Figure 4(a). Wall distribution of entropy (FVG scheme), NACA 0012 ($M_\infty = 0{\cdot}63$, $\alpha = 2°$)

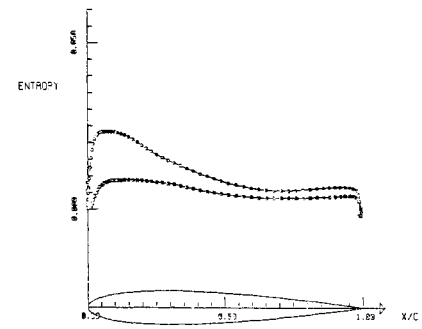

Figure 4(b). Wall distribution of entropy (FVS1 + PSI), NACA 0012 ($M_\infty = 0{\cdot}63$, $\alpha = 2°$)

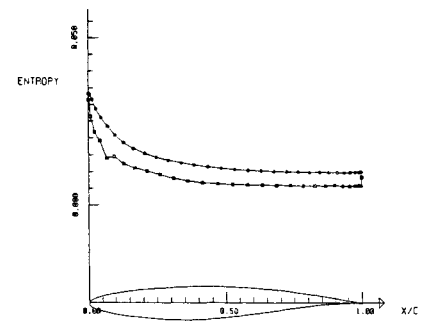

Figure 5(a). Wall distribution of entropy (FVG scheme), RAE 2822 coarse grid ($M_\infty = 0{\cdot}30$, $\alpha = 2°$)

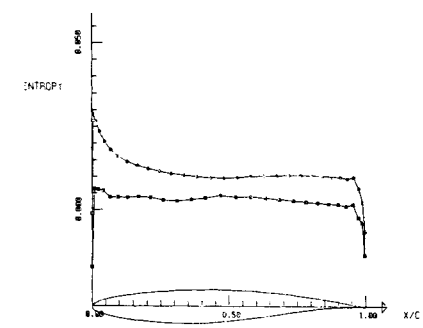

Figure 5(b). Wall distribution of entropy (FVS1 + N), RAE 2822 coarse grid ($M_\infty = 0{\cdot}30$, $\alpha = 2°$)

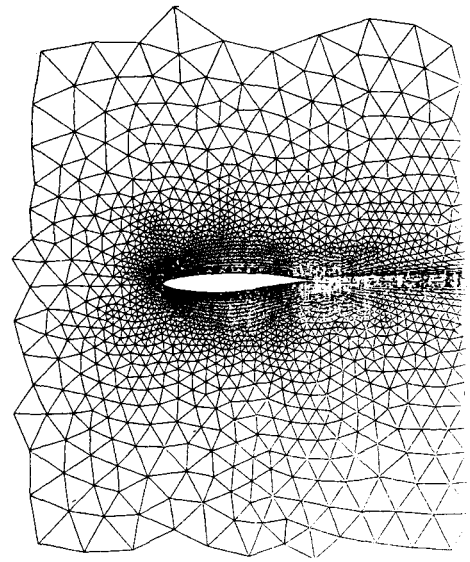

Figure 6. RAE 2822 aerofoil fine grid

the pressure coefficient distribution C_p is comparable for the four simulations. We can notice that the maximum value tends to decrease for the FVS splitting schemes. For the entropy plots the same conclusions as in the previous test case can be made concerning the weak entropy level generated at the windward side by the FVS1 schemes, whereas the leading edge entropy is uniformly convected. The FVS2 and reference schemes give comparable solutions. It is noticeable that the influence of the scalar scheme (N or PSI) on the solution is weak; this could indicate that the dissipation is mostly controlled by the pressure term.

8. CONCLUSIONS

We have investigated the possibility of relying on multidimensional upwinding for inviscid compressible flow simulation by taking advantage of convection/acoustic splitting. The resulting

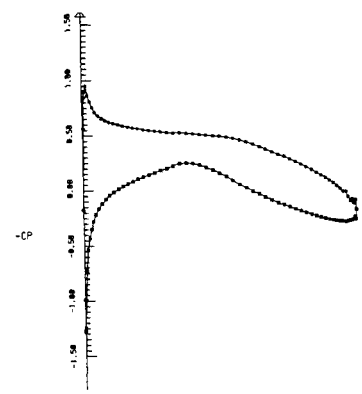

Figure 7(a). Wall distribution of C_p (FVG scheme), RAE 2822 fine grid (M_∞ = 0·30, α = 2°)

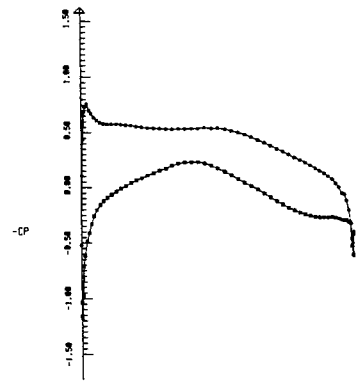

Figure 7(b). Wall distribution of C_p (FVS1 + N), RAE 2822 fine grid ($M_\infty = 0{\cdot}30$, $\alpha = 2°$)

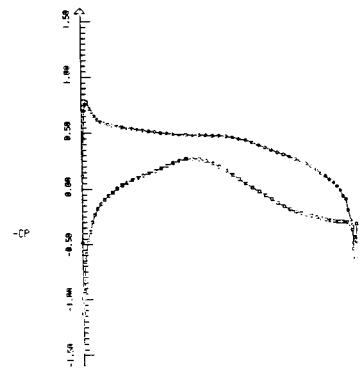

Figure 7(c). Wall distribution of C_p (FVS1 + PSI), RAE 2822 fine grid ($M_\infty = 0{\cdot}30$, $\alpha = 2°$)

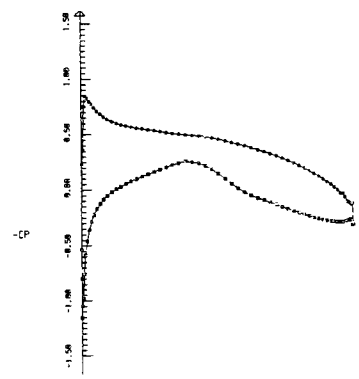

Figure 7(d). Wall distribution of C_p (FVS2 + PSI), RAE 2822 fine grid ($M_\infty = 0{\cdot}30$, $\alpha = 2°$)

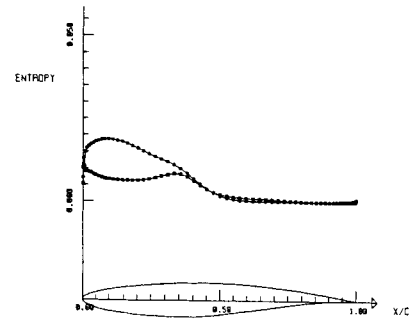

Figure 8(a). Wall distribution of entropy (FVG scheme), RAE 2822 fine grid ($M = 0{\cdot}30$, $\alpha = 2°$)

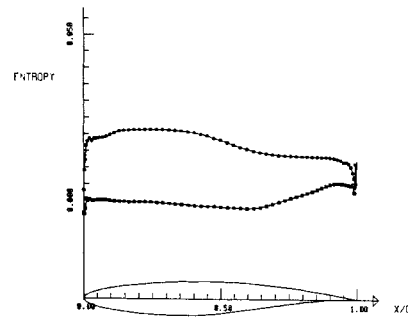

Figure 8(b). Wall distribution of entropy (FVS1 + N), RAE 2822 fine grid ($M_\infty = 0{\cdot}30$, $\alpha = 2°$)

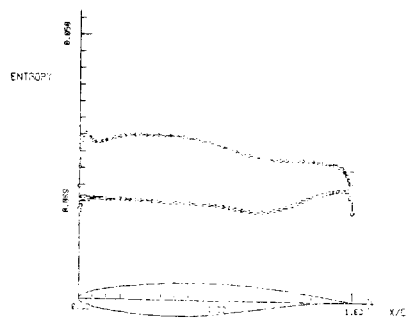

Figure 8(c). Wall distribution of entropy (FVS1 + PSI), RAE 2822 fine grid ($M_\infty = 0{\cdot}30$, $\alpha = 2°$)

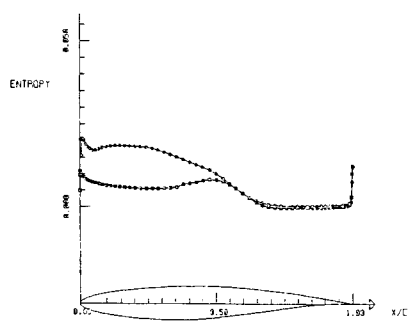

Figure 8(d). Wall distribution of entropy (FVS2 + PSI), RAE 2822 fine grid ($M_\infty = 0{\cdot}30$, $\alpha = 2°$)

schemes have been applied to subsonic flow simulations and compare well with classical upwind schemes. This gives an attractive frame for potential improvements. Further improvements are required in order to achieve a reliable formulation.

1. As reported above, strong conditions have been applied to impose the no-slip condition at the surface. This treatment certainly affects the accuracy of the method. Alternative techniques that could be used have recently been reported in Reference 18.
2. The present treatment of the pressure term is not satisfactory. The approximation still relies on a classical monodimensional upwinding which is certainly responsible for the excessive remaining dissipation as discussed in the previous section. Further investigations to derive a more accurate formulation have to be performed.
3. We have restricted our analysis to subsonic flows. The proposed frame of splitting formulations should handle transonic flows as well.

ACKNOWLEDGEMENTS

The author wants to thank M. Mallet, M. Ravachol and B. Perthame as well as C. Kasbarian for the numerous discussions to understand the different scalar schemes and their links with classical upwinding and SUPG.

REFERENCES

1. T. J. Barth, 'Numerical aspects of computing viscous high Reynolds number flows on unstructured meshes', *AIAA Paper 91-0721*, 1991.
2. L. Fezoui and B. Stoufflet, 'A class of implicit upwind schemes for Euler simulations with unstructured meshes', *J. Comput. Phys.*, **84**, 174–206 (1989).
3. M. P. Leclercq, B. Mantel, J. Periaux, P. Perrier and B. Stoufflet, 'On recent 3-D Euler computations around a complete aircraft using adaptive unstructured mesh refinements', *Proc. Second World Congr. on Computational Mechanics*, Stuttgart, August 1990.
4. B. van Leer, 'Progress in multi-dimensional upwind differencing', *NASA Contractor Report 189708, ICASE Report 92-43*, 1992.
5. R. Struijs, P. L. Roe and H. Deconinck, 'Fluctuation splitting schemes for the 2D Euler equations', *Von Karman Institute LS 1991-01*, 1991.
6. K. G. Powell, B. van Leer and P. L. Roe, 'Towards a genuinely multidimensional upwind scheme', *Von Karman Institute LS 1990-03*, 1990.
7. M. S. Liou, '3-D hypersonic Euler numerical simulation around space vehicles using adapted finite elements', *AIAA Paper 86-0560*, 1986.
8. A. Jameson, '3-D hypersonic artificial diffusion, upwind biasing, limiters and their effect on accuracy and multigrid convergence in transonic and hypersonic flows', *AIAA Paper 93-3359*, 1993.
9. G. S. Ianelli and A. J. Baker, 'An intrinsically *N*-dimensional generalized flux vector splitting implicit finite element Euler algorithm', *AIAA Paper 91-0123*, 1991.
10. F. Angrand, A. Dervieux, L. Loth and G. Vijayasundaram, 'Simulation of Euler transonic flows by means of explicit finite element-type schemes', *INRIA RR 250*, 1983.
11. P. Rostand and B. Stoufflet, 'TVD schemes to compute compressible viscous flows on unstructured meshes', in *Notes on Numerical Fluid Mechanics*, Vol. 24, Vieweg, Braunschweig, 1989, p. 510.
12. A. Dervieux, L. Fezoui and F. Loriot, 'On high resolution variants of Lagrange–Galerkin finite element schemes', *INRIA Report*, 1991.
13. C. Kasbarian, M. P. Leclercq, M. Ravachol and B. Stoufflet, 'Improvements of upwind formulations on unstructured meshes', *Proc. 4th Int. Conf. on Hyperbolic Problems*, April 1992.
14. B. van Leer, 'Computational methods for ideal compressible flow', *Von Karman Institute 1983-04*, 1983.
15. P. Arminjon, A. Dervieux, L. Fezoui, H. Steve and B. Stoufflet, 'Non-oscillatory schemes for multidimensional Euler calculations with unstructured grids', in *Notes on Numerical Fluid Mechanics*, Vol. 24, Vieweg, Braunschweig, 1989, p. 1.
16. B. Stoufflet, J. Periaux, F. Fezoui and A. Dervieux, '3-D hypersonic Euler numerical simulation around space vehicles using adapted fianite elements', *AIAA Paper 86-0560*, 1986.
17. L. Fezoui and A. Dervieux, 'Finite-element non oscillatory schemes for compressible flows', *Proc. Symp. on Computational Mathematics and Applications*, Pavie, October 1989.
18. H. Paillere, H. Deconinck, R. Struijs, P. L. Roe, L. M. Mesaros and J. D. Muller, 'Computations of inviscid compressible flows using fluctuation-splitting on triangular meshes', *AIAA Paper 93-3301*, 1993.